Applied Thermal Engineering 304 (2026) 132751

Contents lists available at ScienceDirect

Applied Thermal Engineering

journal homepage: www.elsevier.com/locate/ate

Research Paper

Thermoelastic effects on material temperature in hydrogen/oxygen premixed flame–material interaction: A numerical study

Chunkan Yu

Institute of Technical Thermodynamics (ITT), Karlsruhe Institute of Technology (KIT), Engelbert-Arnold-Str. 4, Karlsruhe, 76131, Baden Württemberg, Germany

ARTICLE INFO

Keywords:
Hydrogen flame
Transient process
Flame–material interaction
Thermoelasticity
Gough–Joule effect

ABSTRACT

Accurate prediction of the material temperature field during hydrogen flame heating is essential for assessing thermal loading and material integrity. In the present work, a thermo-mechanically coupled numerical model is employed to investigate transient flame–material interaction between a laminar hydrogen/oxygen premixed strained flame and a solid material. Particular attention is paid to the influence of the thermoelastic (Gough–Joule) effect on the material temperature evolution. The results show that the Gough–Joule effect acts as an additional heat source and accelerates the heating process. By using flame with high strain rate, neglecting the Gough–Joule effect results in noticeable error in the predicted time required for the material to reach the yield-strength condition. The relative importance of the Gough–Joule effect is found to increase monotonically with flame strain rate. These findings indicate that thermoelastic coupling can substantially influence transient flame–material interaction under rapid hydrogen-flame heating and should be considered when accurate prediction of the material temperature field is required.

1. Introduction

Hydrogen is widely regarded as one of the most promising carbon-free energy carriers for future energy systems [1,2]. In addition to its role in power generation and propulsion applications, hydrogen combustion is attracting increasing interest in thermal processing technologies due to its high reactivity, clean combustion products and capability of delivering intense heat fluxes [3,4]. As hydrogen-based thermal systems continue to expand, understanding the interaction between hydrogen flames and engineering materials becomes increasingly important for the design, operation and safety assessment of combustion devices. Such study involves e.g. the flame quenching at the presence of wall [5].

The thermal response of materials exposed to hydrogen flames is governed by a complex interaction between combustion, heat transfer and material behavior. Accurate prediction of the resulting temperature field inside the material is of particular importance because temperature directly affects thermal stresses, structural integrity, material degradation and failure mechanisms [6–8]. Despite its practical relevance, the transient interaction between hydrogen flames and solid materials remains considerably less studied than the combustion characteristics of hydrogen flames themselves. Existing studies have primarily focused on flame structure, burning velocity, ignition, extinction and flame stabilization, whereas comparatively limited attention has been devoted to the transient heating process of the material and the resulting thermo-mechanical response.

Recent studies have shown that the thermal and mechanical behavior of a material cannot always be treated independently [9]. Within the framework of thermoelasticity, the balance of internal energy and the balance of linear momentum are intrinsically coupled. Consequently, material deformation can induce a reversible thermal response, commonly referred to as the elasto-caloric effect or Gough–Joule effect. This mechanism introduces an additional contribution to the energy balance and may alter the evolution of the temperature field inside the material. Since the magnitude of the Gough–Joule effect depends on both the deformation rate and the spatial distribution of deformation, its importance is expected to increase under conditions involving rapid heating and strong thermal gradients.

In the previous study [9], the influence of the Gough–Joule effect was investigated for flame–material interaction involving ammonia/hydrogen combustion. It was found that the resulting elastocaloric contribution had only a limited impact on the material temperature field. However, hydrogen flames are characterized by significantly higher reactivity, higher temperature gradients and more rapid heat transfer than ammonia-containing flames. As a consequence, substantially stronger thermo-elastic deformation may develop during hydrogen flame heating, potentially amplifying the associated Gough–Joule effect. Whether this deformation-induced thermal response remains negligible or becomes an important component of the overall energy balance therefore remains an open question.

E-mail address: chunkan.yu@kit.edu.

https://doi.org/10.1016/j.applthermaleng.2026.132751
Received 14 June 2026; Received in revised form 25 July 2026; Accepted 6 August 2026
Available online 13 August 2026

The objective of the present work is to investigate the importance of the Gough–Joule effect during transient heating of a solid material by hydrogen premixed flames. To achieve this goal, a canonical flame–material interaction configuration based on a laminar premixed strained hydrogen/oxygen flame is considered. The study first examines the fundamental heating characteristics of the material under different flame strain rates and subsequently quantifies the influence of thermoelastic coupling on the predicted temperature evolution. Particular attention is paid to the role of flame strain rate, heating rate, temperature gradients and deformation-induced thermal effects. Through this analysis, the present work aims to provide a more accurate description of the material temperature field during hydrogen flame heating and to assess the conditions under which the Gough–Joule effect must be considered in flame–material interaction problems. It should be noted that the term flame–material interaction is intentionally used throughout this work. Unlike the conventional concept of flame–wall interaction, which primarily concerns the influence of a wall on flame behavior, the present study focuses on the transient thermal and thermo-mechanical response of the solid material subjected to flame heating. Therefore, the material itself, rather than the wall as a boundary condition, constitutes the primary object of investigation.

2. Mathematical modeling

2.1. Model configuration

The computational configuration considered in the present work is illustrated in Fig. 1. The study is based on a one-dimensional laminar premixed strained flame established between two opposed streams of unburned mixture. This canonical configuration has been extensively used in fundamental combustion studies because it provides a well-defined and controllable flame strain rate while keeping the essential characteristics of flame structure and extinction behavior. This configuration has also been extensively investigated under transient conditions using analytical approaches [10,11], providing valuable insight into the underlying combustion physics.

As shown in Fig. 1(a), two identical premixed streams flow toward each other and form a symmetric counterflow flame. The stagnation plane is located at the center of the domain ($z = 0$). The flame strain rate is controlled through the inlet flow velocity conditions and serves as the primary parameter characterizing the aerodynamic stretching imposed on the flame.

To investigate the transient flame–material interaction, a plane wall of thickness δ is subsequently introduced at the stagnation plane, as illustrated in Fig. 1(b). Due to the symmetry of the configuration, identical flames are formed on both sides of the wall. Meanwhile, energy is transferred from the flame to the solid surface, resulting in a transient heating process inside the material.

Such configuration provides a simplified yet representative framework for investigating the coupled interaction between combustion, heat transfer and thermal response. In particular, it allows the influence of flame strain rate on material heating and deformation-induced thermal effects to be systematically isolated and quantified. Heat transfer between the reacting flow and the solid material is treated as a conjugate heat transfer problem. The energy equations are solved simultaneously in both domains, while continuity of temperature and heat flux is imposed at the flame–material interface. Additional thermal and mechanical boundary conditions can also be found in [9] in details.

In the following, the governing equations for both systems and their coupling will be briefly outlined.

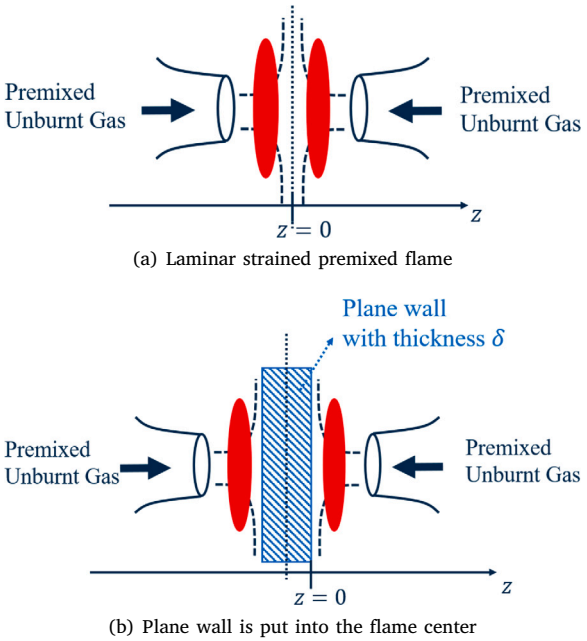

(a) Laminar strained premixed flame

(b) Plane wall is put into the flame center

Fig. 1. Schematic illustration of the computational configuration considered in the present study. (a) Laminar premixed strained flame established between two opposed premixed streams. (b) Flame–material interaction configuration, where a plane wall of thickness δ is placed at the stagnation plane and heated up.

2.2. Governing equations

The mathematical framework used in the present study is identical to that presented in the recent work [9,12], where the complete governing equations and numerical implementation are described in detail. Therefore, in the present work only the principal equations and the physical models most relevant to the present discussion are summarized here, while the interested reader is referred to [9] for the complete mathematical formulation. The governing equations of the gas phase and the solid are solved in a fully coupled manner, forming a conjugate heat transfer problem across the flame–material interface. In addition, the present study is restricted to a one-dimensional configuration, i.e., all governing fields, including temperature, species concentrations in the reacting flow, and mechanical deformation in the solid, are assumed to vary only in the direction normal to the flame–material interface.

2.2.1. Laminar premixed flame

The combustion simulations are based on the two-parameter formulation proposed by Stahl and Warnatz [13], in which the tangential pressure gradient J and the tangential velocity gradient G are used to characterize the strained flame configuration. From the tangential pressure gradient, the flame strain rate can be defined as

$$a = \sqrt{-J/\rho_{\mathrm{ub}}}, \tag{1}$$

where ρ_{ub} denotes the density of the unburned mixture. The flame strain rate characterizes the velocity gradient acting on the flame front and serves as a measure of the aerodynamic stretching imposed on the flame [14,15]. Consequently, larger flow velocities correspond to larger flame strain rates .

The combustion formulation is identical to that presented in [9] and accounts for differential diffusion among species, thermal diffusion (Soret effect) [16]. Detailed chemical kinetics are used to accurately capture the combustion chemistry of the hydrogen/oxygen system. In

addition, heterogeneous surface reactions occurring at the material interface are included and will be described later.

For the energy equation, volumetric radiative heat losses are also considered. In the present work, thermal radiation is modeled using the optically thin approximation model (OTM) [17]. More sophisticated radiation models, such as the discrete ordinates method (DOM) [18,19], could also be considered. However, previous investigations [9] have shown that radiative heat transfer contributes only negligibly to the overall energy exchange at the flame–material interface. Instead, the thermal loading of the material is mainly dominated by conductive heat transfer from the flame. Consequently, the material temperature evolution and the associated thermo-elastic response are controlled almost entirely by conductive heat flux. Under such conditions, the choice of radiation model has virtually no influence on the quantities of interest considered in the present work. Therefore, although the OTM provides a simplified description of radiative heat transfer, its use does not affect the predicted flame–material interaction behavior, and the more expensive DOM model would lead to essentially identical results.

2.2.2. Thermoelastic solid model

The thermoelastic formulation used in the present work has been described in detail in previous studies [9]. The material is modeled as an isotropic thermoelastic solid undergoing small deformations. Under these assumptions, the balance equations for internal energy and linear momentum can be written as

$$\rho_0 c_\epsilon \dot{T} = -\mathrm{div}(\mathbf{q}) - T\boldsymbol{\beta}\cdot\dot{\boldsymbol{\varepsilon}}, \tag{2}$$

and

$$\rho_0 \ddot{\mathbf{u}} = \mathrm{div}(\boldsymbol{\sigma}), \tag{3}$$

where ρ_0 is the material density, c_ϵ is the specific heat capacity at constant strain, T is the temperature, $\mathbf{q}$ is the heat flux, $\mathbf{u}$ denotes the displacement vector, $\boldsymbol{\sigma}$ is the Cauchy stress tensor, and $\boldsymbol{\varepsilon}$ is the infinitesimal strain tensor. $\boldsymbol{\beta}$ is the coefficient of thermal stress, and can be calculated as the following for isotropic thermo-elastic materials [9]:

$$\begin{aligned}\boldsymbol{\beta}(T) &= 3K(T)\alpha(T)\boldsymbol{I} - 2G'(T)\boldsymbol{\varepsilon}^{\mathrm{dev}} \\ &\quad + 3K'(T)\left(\int_{T_0}^{T}\alpha\left(\tilde{T}\right)\mathrm{d}\tilde{T}\,\boldsymbol{I} - \boldsymbol{\varepsilon}^{\mathrm{sph}}\right),\end{aligned} \tag{4}$$

in which K and G are the bulk modulus and shear modulus, and $K' = \mathrm{d}K/\mathrm{d}T$ and $G' = \mathrm{d}G/\mathrm{d}T$ the corresponding derivative with respect to temperature. α is the coefficient of thermal expansion and a scalar due to isotropy. And $\boldsymbol{\varepsilon}^{\mathrm{sph}}$ and $\boldsymbol{\varepsilon}^{\mathrm{dev}}$ are the spherical and deviatoric part of the strain tensor as $\boldsymbol{\varepsilon}^{\mathrm{sph}} = 1/3\,\mathrm{tr}(\boldsymbol{\varepsilon})\boldsymbol{I}$ and $\boldsymbol{\varepsilon}^{\mathrm{dev}} = \boldsymbol{\varepsilon} - \boldsymbol{\varepsilon}^{\mathrm{sph}}$.

A key feature of Eq. (2) is the thermo-mechanical coupling term $T\boldsymbol{\beta}\cdot\dot{\boldsymbol{\varepsilon}}$, which couples the balance of internal energy with the balance of linear momentum. Consequently, deformation of the material can directly affect the local temperature field through an elasto/caloric response. This phenomenon is commonly referred to as the Gough–Joule effect and constitutes the primary focus of the present study. Physically, the term $T\boldsymbol{\beta}\cdot\dot{\boldsymbol{\varepsilon}}$ represents a reversible conversion between mechanical and thermal energy. Depending on the local deformation state, this coupling term may act either as a heat source or as a heat sink in the energy equation. Therefore, the temperature evolution inside the material is not governed solely by heat conduction from the flame, but also by the transient thermo/elastic deformation induced by the highly non-uniform temperature field. Under rapid heating conditions, significant deformation rates and deformation gradients may develop, leading to a non-negligible contribution of the Gough–Joule effect to the overall energy balance.

Similar to the combustion formulation, the present flame–material interaction problem is treated as one-dimensional. Therefore, all thermomechanical quantities depend only on the spatial coordinate normal to the material surface, i.e., the z-coordinate. As a result, both the temperature field and the displacement field are functions of z and time only. Under this assumption, the strain tensor reduces to a single non-zero normal component, and the resulting thermoelastic problem becomes effectively one-dimensional.

2.3. Reactions in gas-phase and at the wall surface

In the present work, the chemical mechanism including surface reactions is adopted from [20]. Additionally, five recombination/destruction reactions of reactive species at the wall surface are considered:

(S1) $\mathrm{HO_2} \xrightarrow{\text{wall}} 0.5\mathrm{H_2O} + 0.75\mathrm{O_2}$

(S2) $\mathrm{O} \xrightarrow{\text{wall}} 0.5\mathrm{O_2}$

(S3) $\mathrm{H} \xrightarrow{\text{wall}} 0.5\mathrm{H_2}$

(S4) $\mathrm{OH} \xrightarrow{\text{wall}} 0.5\mathrm{H_2O} + 0.25\mathrm{O_2}$

(S5) $\mathrm{H_2O_2} \xrightarrow{\text{wall}} \mathrm{H_2O} + 0.5\mathrm{O_2}$

These surface reactions are identical to those employed in [20,21]. It should be emphasized that, for the present flame–material interaction problem, the specific stable products formed following radical destruction at the wall are not of primary importance. The dominant role of the surface chemistry is the removal of reactive radicals from the gas phase, thereby reducing the local radical pool available for chain-branching reactions and modifying the overall flame behavior. Consequently, the heating process is governed primarily by the radical destruction rate at the surface rather than by the particular stable species generated. Numerical experiments confirm that alternative formulations producing the same radical consumption rate lead to essentially identical results. For example, replacing $\mathrm{HO_2} \xrightarrow{\text{wall}} 0.5\mathrm{H_2O}+0.75\mathrm{O_2}$ with $\mathrm{HO_2} \xrightarrow{\text{wall}} 0.5\mathrm{H_2}+\mathrm{O_2}$ results in virtually identical predictions of flame behavior and material heating. Therefore, the conclusions presented in this work are insensitive to the detailed specification of the stable products appearing in the surface reaction mechanism.

2.4. Material properties

The material considered in the present study is Inconel 718, which is identical to that employed in [9]. The primary reason for this choice is that a complete set of thermo-elastic material properties is available over a wide temperature range, with all properties represented by thermodynamically consistent temperature-dependent polynomial functions. Such a formulation ensures that the constitutive model remains thermodynamically admissible throughout the temperature range encountered during flame-induced heating.

Note that all thermo-elastic material properties are treated as temperature dependent. These include the thermal conductivity $k(T)$ (in unit W/m·K) as

$$k(T) = 0.01824\,\frac{T}{\mathrm{K}} + 4.407, \tag{5}$$

the coefficient of thermal expansion $\alpha(T)$ (in unit 1/K) as

$$\alpha(T) = 5.23\cdot 10^{-9}\,\frac{T}{\mathrm{K}} + 1.127\cdot 10^{-5}, \tag{6}$$

the bulk modulus $K(T)$ (in unit GPa) as

$$K(T) = -0.046\,\frac{T}{\mathrm{K}} + 173.36, \tag{7}$$

and the shear modulus $G(T)$ (in unit GPa) as

$$K(T) = -0.0178\,\frac{T}{\mathrm{K}} + 83.17. \tag{8}$$

These polynomial representations were obtained in [9] through a thermodynamically consistent fitting procedure and are valid over the temperature range of 300–650 K. This range corresponds to the thermoelastic regime considered in the present study. At temperatures above approximately 650 K, the material enters the plastic deformation regime, for which the present thermoelastic constitutive model is no longer applicable. Therefore, all quantitative analyses are restricted to temperatures below 650 K.

2.5. Numerical implementation

The numerical simulations were performed using the in-house combustion code INSFLA [20], which has been extensively developed and validated in previous studies. Within INSFLA, the governing equations are solved using the method-of-lines approach. The spatial derivatives are discretized by finite difference schemes, thereby transforming the governing partial differential equations into a system of ordinary differential equations. The resulting equations are then integrated in time using the numerical time-integration algorithms implemented in INSFLA. The combustion and thermoelastic equations are solved in a fully coupled manner through the conjugate heat transfer conditions imposed at the flame–material interface.

3. A-priori study on hydrogen/oxygen premixed strained flame

The interaction between hydrogen premixed flames and solid materials is inherently governed by the coupled behavior of combustion, heat transfer, and solid response. In such systems, the thermal and mechanical state of the material is strongly influenced by the local flame structure. Therefore, prior to investigating flame–material interaction, it is essential to provide a clear understanding of the fundamental properties of the underlying combustion system. Given that the general behavior of strained premixed flames has been well documented such as in [22–24], the present section does not aim to provide a comprehensive review. Instead, it focuses on the key combustion characteristics that are most relevant to subsequent analysis of flame–material interaction, which will be discussed in the following section.

Fig. 2 summarizes the fundamental response of the hydrogen/oxygen premixed strained flame to variations in flame strain rate. As shown in the upper subfigure, the flame peak temperature decreases monotonically with increasing strain rate. This behavior is associated with the enhanced aerodynamic stretching imposed on the flame, which reduces the residence time available for chemical reaction. As the strain rate approaches a critical value, the flame reaches the extinction limit. Beyond this point, a further increase in strain rate leads to flame quenching.

The lower subfigure further illustrates the modification of flame structure under different strain conditions through the corresponding temperature spatial profiles. With increasing strain rate, the reaction zone clearly shifts toward a thinner spatial region, indicating a significant reduction in flame thickness. Such flame compression is a characteristic feature of strained premixed flames and directly influences the local thermal gradients near the flame front.

For the present flame–material interaction problem, these observations are particularly important because both the magnitude and localization of thermal energy deposition strongly affect the subsequent thermoelastic response of the material. In particular, the narrowing of the flame zone under high-strain conditions may induce steeper temperature gradients within the solid, thereby modifying the coupled thermomechanical response associated with the elasto-caloric effect (Gough–Joule effect).

4. Results and discussion

Prior to discussing elasto-caloric effects in the material, it is necessary to distinguish between failed and successful heating during flame–solid interaction. Such discussion is essential because the existence of a stable heating process is a prerequisite for any meaningful analysis of deformation-induced thermal effects associated with the Gough–Joule effect.

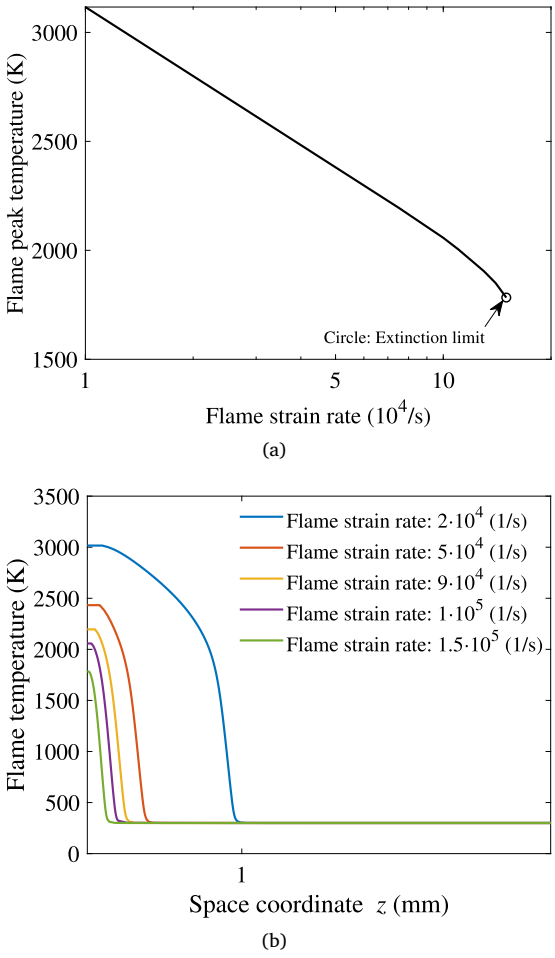

Fig. 2. Effects of flame strain rate on hydrogen/oxygen premixed strained flames. Upper: variation of flame peak temperature with strain rate and the corresponding extinction limit. Lower: flame temperature spatial profiles under different strain rates.

4.1. Failed heating

Fig. 3 illustrates a representative failed heating process during flame–solid interaction at a relatively high strain rate. Prior to interaction with the solid surface ($t < 0$), the flame maintains a stable reaction zone characterized by a localized high-temperature region. Once the flame interacts with the solid ($t \geq 0$), however, substantial heat is rapidly extracted from the reacting flow due to thermal conduction into the colder material. This additional heat loss strongly modifies the flame structure and progressively weakens the reaction zone.

As shown in the upper sub-figure, the flame temperature decreases continuously after interaction with the solid. Eventually, the flame can no longer sustain combustion process and undergoes extinction. The corresponding temporal evolution shown in the lower sub-figure further supports this process. The peak flame temperature decays monotonically and experiences a rapid drop within a very short time. In contrast, the temperatures inside the solid increase only slightly throughout the interaction process, indicating that the flame is extinguished before significant thermal energy can be deposited into the material.

This failed heating behavior originates from the competition between flame heat release and heat losses imposed by the solid. For strained premixed flames, increasing strain rate enhances aerodynamic stretching and reduces the characteristic chemical reaction time. As a result, the flame becomes increasingly sensitive to external thermal

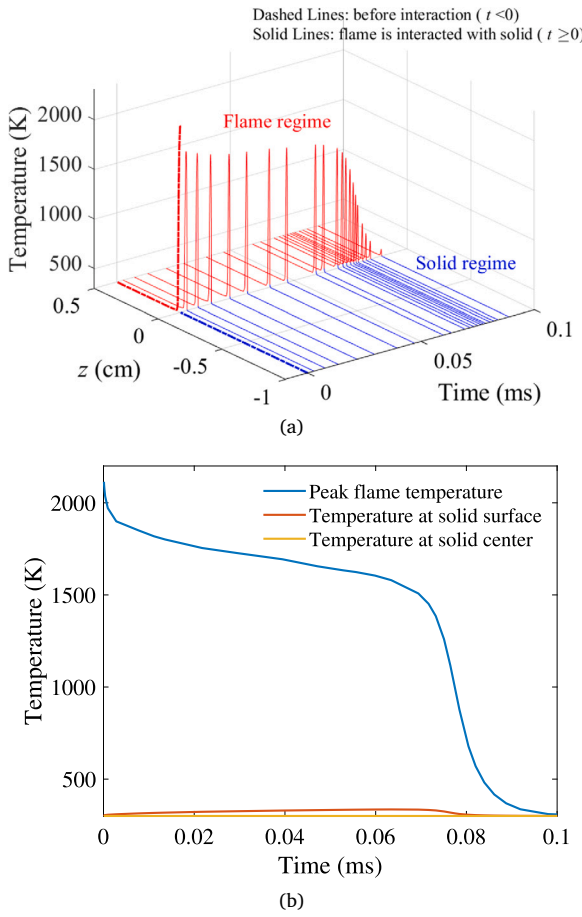

Fig. 3. Temporal evolution of flame–material interaction under failed heating conditions at a flame strain rate of $a = 8 \cdot 10^4(1/s)$. Upper: evolution of the temperature field before and after flame interaction with the solid surface. Lower: temporal evolution of the peak flame temperature, the solid surface temperature and the solid center temperature.

perturbations. Under such conditions, the additional conductive heat loss toward the solid reduces the local flame temperature and weakens the chemical reaction rate to a level insufficient to counter-balance the imposed flow strain. Consequently, the flame undergoes the quenching process.

The existence of failed heating is less interesting for the present study because the maximum temperature rise inside the solid remains below approximately 50 K throughout the interaction process, as shown in Fig. 3(lower). Consequently, the induced thermal deformation inside the material is expected to be extremely small. Since the Gough–Joule effect originates from the coupling between deformation and thermal response, such weak thermo-mechanical deformation leads to the fact that the influence of the Gough–Joule effect can reasonably be neglected.

4.2. Successful heating

4.2.1. General observation of the heating process

Fig. 4 illustrates a representative successful heating process during flame–material interaction at flame strain rate $a = 7 \cdot 10^4$ (1/s). Unlike the failed heating case discussed previously, the flame remains self-sustained after interacting with the solid surface despite the additional conductive heat losses introduced by the material. As shown in the upper sub-figure, although the flame structure is modified during interaction, a stable high-temperature reaction zone persists throughout the heating process, allowing continuous thermal energy transfer from the flame to the solid.

The lower sub-figure further shows the temporal evolution of the thermal response inside the material. Following flame interaction, the solid surface temperature increases continuously and approaches the melting point of the material. In contrast, the temperature at the solid center remains nearly unchanged during the entire process. Meanwhile, the evolution of the peak flame temperature indicates that the flame adapts to the additional heat loss imposed by the solid without undergoing extinction.

Two different regimes can further be identified in the lower sub-figure. The solid-line region corresponds to conditions where the maximum von Mises stress (σ_v) inside the material remains below the yield strength (σ_Y), such that the material response is primarily thermo-elastic. In contrast, the dashed-line region denotes the regime where the von Mises stress (σ_v) exceeds the yield strength (σ_Y) while the surface temperature continues increasing toward the melting point. Two important points need to be mentioned explicitly:

- The temperature rise at the material surface occurs extremely rapidly, primarily within the millisecond timescale immediately following flame interaction. This indicates highly localized and intense thermal loading from the flame.
- Despite the rapid heating near the surface, the temperature at the material center remains almost unaffected throughout the considered time interval, because the surface is heated much more rapidly than heat can be conducted into the interior of the material.

These observations are particularly important for the present study of elasto-caloric effects (Gough–Joule effect) inside the material. The Gough–Joule effect is closely related not only to the magnitude of thermal deformation, but also to both the temporal rate of deformation evolution and the spatial gradients of deformation within the material. The present successful heating case clearly shows both rapid temporal variations and strong spatial non-uniformity in the thermal field. Consequently, significant thermomechanical coupling may develop inside the material, suggesting that the Gough–Joule effect can become important under successful heating conditions, which will be discussed in details in the following.

It should also be emphasized that the present work is formulated within the framework of thermoelasticity. Therefore, the following discussions are restricted to the regime in which the maximum von Mises stress remains below the material yield strength, such that irreversible plastic deformation is not considered, which needs additional mathematical modeling.

4.2.2. Effect of flame strain rate on the heating process

Before discussing further the Gough–Joule effect on the prediction of material temperature, it is interesting to investigate how the flame strain rate imposed on the combustion system could potentially affect the heating process in a general way.

Fig. 5 shows the temporal evolution of the material surface temperature under different flame strain rates. Each curve corresponds to a successful heating case and ends at the timepoint when the maximum von Mises stress inside the material reaches the yield strength limit. It is interesting to see that although lower flame strain rates generally correspond to higher flame temperatures, the heating process is found to be significantly faster at higher strain rates. In particular, the material surface temperature increases more rapidly as the strain rate increases, despite the reduction in peak flame temperature discussed previously. This behavior indicates that the heating rate is not governed solely by the flame temperature itself, but also strongly depends on the flame structure and the associated heat transfer characteristics. As discussed in the previous section, increasing flame strain rate leads to a thinner reaction zone and shifts the high-temperature region closer

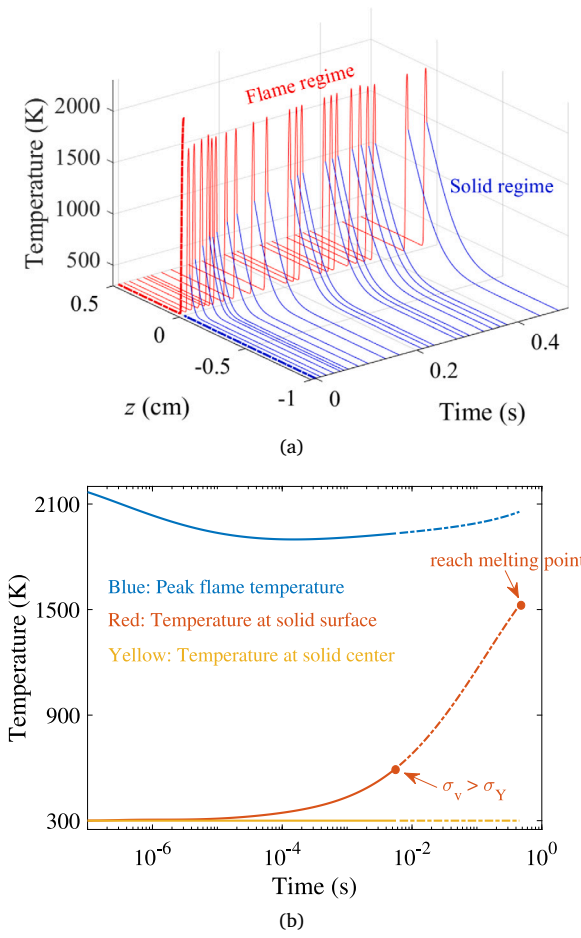

Fig. 4. Temporal evolution of flame–material interaction under successful heating conditions at a flame strain rate of $a = 7 \cdot 10^4 (1/s)$. Upper: evolution of the temperature field before and after flame interaction with the solid surface. Lower: temporal evolution of the peak flame temperature, the solid surface temperature and the solid center temperature.

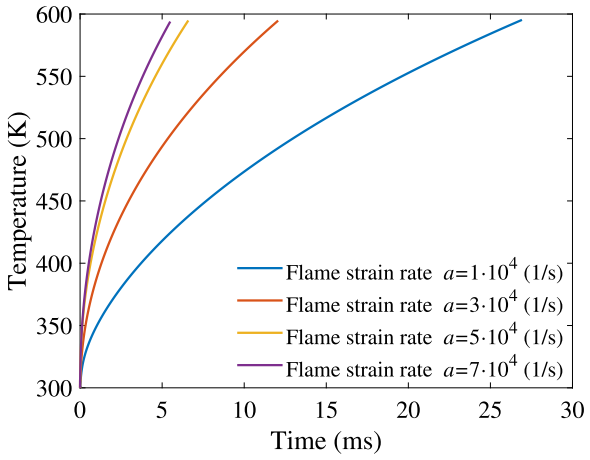

Fig. 5. Temporal evolution of the material surface temperature under different flame strain rates during successful heating. Each curve ends at the timepoint when the maximum von Mises stress inside the material reaches the yield strength.

to the material surface. Consequently, the temperature gradient near the flame front becomes higher, resulting in stronger conductive heat flux from the flame toward the solid. Therefore, even though the flame temperature decreases under higher strain conditions, the enhanced thermal localization and higher gradients result in a more efficient heating process.

However, Fig. 5 only illustrates the temporal evolution of temperature at the material surface. Since the Gough–Joule effect is closely related not only to time evolution itself but also to the spatial gradients of deformation, it is necessary to further examine the spatial distribution of temperature inside the material.

Fig. 6 therefore presents the spatio-temporal evolution of the temperature field inside the material for two representative strain rates. It should be noted that the temporal ranges (y-axis) shown in the two sub-figures are different because the characteristic heating times vary significantly with flame strain rate. In addition, only the near-surface region ($0.8\ \text{cm} \leq z \leq 1\ \text{cm}$) is displayed in order to better visualize the thermal penetration behavior. The temperature in the remaining interior region of the material remains approximately at the initial temperature of 300 K and is essentially unaffected by flame heating during the considered time interval.

The results shown in Fig. 6 indicate an important feature of the heating process. Under high flame strain rate conditions, the heating process occurs so rapidly that thermal conduction does not have sufficient time to transport heat deep into the material interior. Consequently, the thermally affected region remains highly localized near the material surface. In contrast, lower strain rates correspond to slower heating processes, allowing thermal diffusion to penetrate further into the material and producing a broader temperature distribution.

These observations suggest that increasing flame strain rate not only accelerates the heating process, but also generates substantially larger temperature gradients inside the material. Since thermal deformation is directly associated with the temperature field, stronger deformation gradients are likewise expected under high flame strain rate conditions. Such conditions are particularly relevant for the present study because the Gough–Joule effect is coupled to both the magnitude and spatial non-uniformity of thermo-elastic deformation.

4.2.3. Role of the gough–joule effect during flame-induced heating

Fig. 7 compares the temporal evolution of the material surface temperature obtained with and without accounting for the Gough–Joule effect at a flame strain rate of $a = 7 \times 10^4\ \text{s}^{-1}$. Since the material surface is directly exposed to the flame, it represents the hottest location within the solid and therefore provides a convenient measure for assessing the influence of this elasto-caloric effects. It should be noted that the comparison shown in Fig. 7 is restricted to the thermo-elastic regime. The simulations are terminated when the maximum von Mises stress inside the material reaches the yield strength, beyond which plastic deformation is expected to occur and the constitutive equations used in the present thermo-elastic model are no longer applicable. Therefore, the observed temperature difference and heating-time deviation arise solely from thermoelastic coupling and the associated Gough–Joule effect.

Both simulations show a similar overall heating trend, indicating that the primary energy input remains governed by heat transfer from the flame. However, a systematic temperature difference develops throughout the heating process when the Gough–Joule effect is included. The material surface temperature predicted with thermo-elastic coupling is consistently higher than that obtained when the Gough–Joule effect is neglected.

As heating progresses, the discrepancy between the two predictions accumulates. As zoomed in the inset, the temperature difference reaches approximately 17 K during the later stage of heating, corresponding to a relative deviation of approximately 3.17%. Although this difference appears not noticeable when compared with the absolute temperature level, its impact on the heating dynamics is considerably more significant. Specifically, the exclusion of the Gough–Joule effect

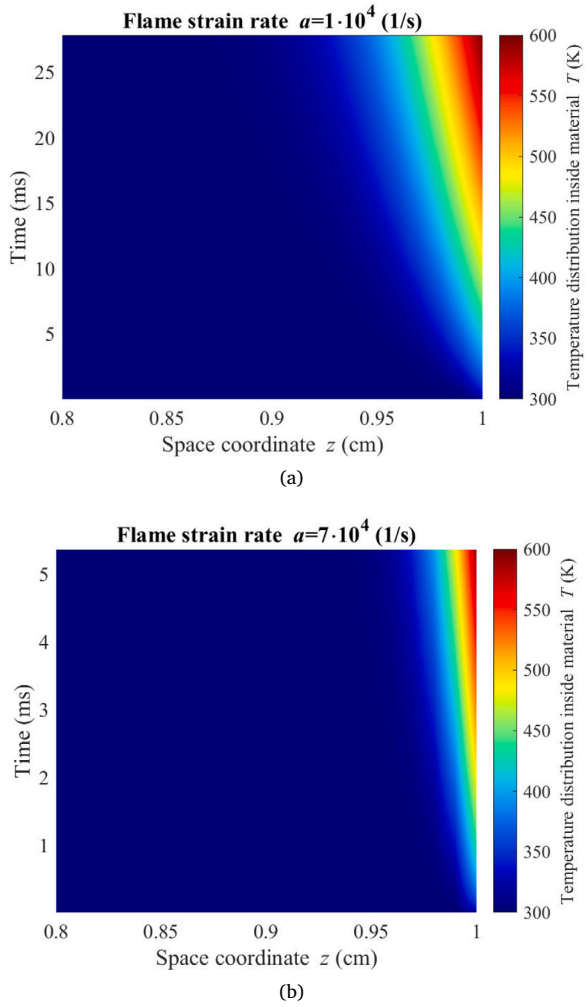

Fig. 6. Spatio-temporal evolution of the temperature field inside the material under successful heating conditions for two representative flame strain rates: (upper) $a = 1 \times 10^4$ $(1/s)$ and (lower) $a = 7 \times 10^4$ $(1/s)$. Only the near-surface region is shown in order to show the thermal penetration behavior inside the material.

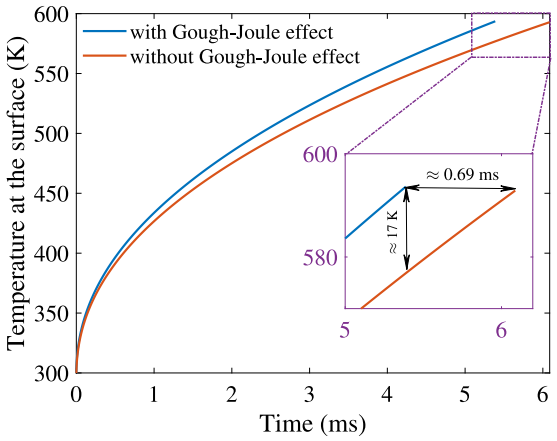

Fig. 7. Influence of the Gough–Joule effect on the evolution of material surface temperature during flame-induced heating at a flame strain rate of $a = 7 \times 10^4$ s^{-1}. The inset provides a magnified view of the temperature difference induced by the elasto-caloric response.

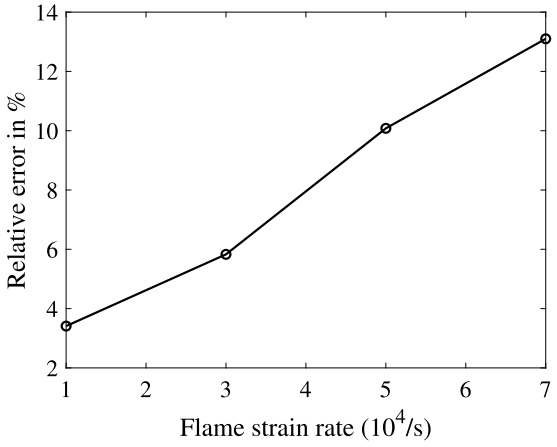

Fig. 8. Relative error in the predicted time required for the maximum von Mises stress to reach the material yield strength when the Gough–Joule effect is neglected, as a function of flame strain rate. The relative error in % here is defined as $100 \times \left| f_{\text{without}} / f_{\text{with}} - 1 \right|$.

slows down the heating process by approximately 0.69 ms, which corresponds to nearly 13% of the total heating time required to reach the same temperature level.

In order to further assess the overall importance of the Gough–Joule effect under different flame strain rates, Fig. 8 presents the relative error in the predicted time required for the maximum von Mises stress to reach the material yield strength when the Gough–Joule effect is neglected.

A clear monotonic increase of the relative error with flame strain rate can be observed. At relatively low strain rates, the heating process proceeds more slowly and the resulting temperature gradients inside the material remain moderate. Consequently, the associated relative slow thermo-elastic deformation leads to relatively small deformation rates, $\dot{\varepsilon}$. Under such conditions, the elasto-caloric contribution arising from the Gough–Joule effect remains weak, and neglecting this mechanism introduces only a minor deviation in the predicted heating dynamics.

In contrast, increasing flame strain rate substantially accelerates the heating process while simultaneously generating stronger temperature gradients inside the material, as discussed in the previous section. Both effects promote more rapid and spatially non-uniform thermo-elastic deformation, resulting in larger values of $\dot{\varepsilon}$. Since the Gough–Joule effect is directly coupled to the evolving deformation field, its contribution becomes increasingly significant under high flame strain rate conditions. Consequently, neglecting the Gough–Joule effect leads to larger errors in predicting the time required for the material to reach its yield-strength limit.

5. Conclusions

The present work investigated the transient interaction between a laminar hydrogen/oxygen premixed strained flame and a thermoelastic solid, with particular emphasis on the role of the Gough–Joule effect in the prediction of the material temperature field. The results showed that the heating outcome is strongly governed by the flame strain rate. While increasing strain rate reduces the flame temperature, it simultaneously enhances heat transfer to the material due to the thinner flame structure and steeper temperature gradients. Consequently, higher strain rates promote more rapid heating and generate stronger thermal gradients inside the solid. These thermal gradients induce significant thermoelastic deformation and deformation rates. The resulting thermo-mechanical coupling acts as an additional contribution

to the material energy balance and accelerates the heating process. Furthermore, the importance of the Gough–Joule effect is found to increase with flame strain rate, indicating a close connection between flame structure, heating dynamics and elastocaloric response.

Overall, the present results show that the Gough–Joule effect can become an important mechanism during rapid hydrogen-flame heating and should be considered when accurate prediction of transient material temperature fields is required. More broadly, the study highlights the necessity of accounting for thermo-mechanical coupling in flame–material interaction problems involving strong thermal gradients and rapid heating processes.

Although the present study is entirely numerical, it is intended to provide the first insight into the potential importance of thermoelastic coupling during hydrogen flame heating. It is expected that the present findings will motivate future experimental investigations to validate the predicted thermoelastic response and the associated Gough–Joule effect. Furthermore, the present study is restricted to a one-dimensional laminar counterflow configuration, which enables the fundamental influence of the Gough–Joule effect to be isolated and quantified. Future work will extend the present thermoelastic framework to multidimensional and turbulent hydrogen flame configurations in order to assess the applicability of the present conclusions under practical flame–material interaction conditions.

Declaration of competing interest

The authors declare that they have no known competing financial interests or personal relationships that could have appeared to influence the work reported in this paper.

Acknowledgment

Author acknowledges financial support by the DFG (project H2MAT3D, project number 523879740 within the DFG-SPP 2419 HyCAM).

Data availability

Data will be made available on request.

References

[1] P. Su-Ungkavatin, L. Tiruta-Barna, L. Hamelin, Biofuels, electrofuels, electric or hydrogen?: A review of current and emerging sustainable aviation systems, Prog. Energy Combust. Sci. 96 (2023) 101073.
[2] M.A. Rosen, S. Koohi-Fayegh, The prospects for hydrogen as an energy carrier: An overview of hydrogen energy and hydrogen energy systems, Energy Ecol. Environ. 1 (1) (2016) 10–29.
[3] J. Li, H. Huang, N. Kobayashi, Hydrogen combustion as a thermal source, Energy Procedia 142 (2017) 1083–1088.
[4] M. Mayrhofer, M. Koller, P. Seemann, R. Prieler, C. Hochenauer, Assessment of natural gas/hydrogen blends as an alternative fuel for industrial heat treatment furnaces, Int. J. Hydrog. Energy 46 (41) (2021) 21672–21686.
[5] Y. Luo, C. Strassacker, X. Wen, Z. Sun, U. Maas, C. Hasse, Strain rate effects on head-on quenching of laminar premixed methane-air flames, Flow Turbul. Combust. 106 (2) (2021) 631–647.
[6] A.G. Evans, Overview No. 125 design and life prediction issues for high-temperature engineering ceramics and their composites, Acta Mater. 45 (1) (1997) 23–40.
[7] C.J. Middleton, R. Timmins, R.D. Townsend, The integrity of materials in high temperature components; Performance and life assessment, Int. J. Press. Vessels Pip. 66 (1–3) (1996) 33–57.
[8] R. Viswanathan, J. Stringer, Failure mechanisms of high temperature components in power plants, J. Eng. Mater. Technol. 122 (3) (2000) 246–255.
[9] C. Yu, F. Hille, T. Böhlke, M. Fischlschweiger, Thermodynamic consistent modeling of flame–solid interaction and thermo-mechanical response of high-temperature materials, Therm. Sci. Eng. Prog. 75 (2026) 104770.
[10] M.F. Farahani, S. Akbari, S. Sadeghi, M. Bidabadi, M.G. Moghadam, F. Xu, Analytical study of transient counter-flow non-premixed combustion of biomass in presence of thermal radiation, Renew. Energy 159 (2020) 312–325.
[11] M.F. Farahani, S. Akbari, K. Hosseinzadeh, Evaluation of thermal radiation and lewis number effects on oscillatory thermal-diffusive instabilities of counterflow premixed flame fed with moisty biomass particles, Case Stud. Therm. Eng. 58 (2024) 104369.
[12] C. Yu, S. Srikanth, T. Böhlke, B. Gorr, U. Maas, Steady laminar stagnation flow NH3-H2-air flame at a plane wall: Flame extinction limit and its influence on the thermo-mechanical stress and corrosive behavior of wall materials, Appl. Energy Combust. Sci. 18 (2024) 100261.
[13] G. Stahl, J. Warnatz, Numerical investigation of time-dependent properties and extinction of strained methane- and propane-air flamelets, Combust. Flame 85 (3–4) (1991) 285–299.
[14] J.D. Buckmaster, G.S.S. Ludford, Lectures on Mathematical Combustion, SIAM, 1983.
[15] F.A. Williams, Combustion Theory, CRC Press, 2018.
[16] J.O. Hirschfelder, C.F. Curtiss, R.B. Bird, M.G. Mayer, Molecular Theory of Gases and Liquids, vol. 165, Wiley New York, 1964.
[17] Y. Ju, H. Guo, K. Maruta, F. Liu, On the extinction limit and flammability limit of non-adiabatic stretched methane–air premixed flames, J. Fluid Mech. 342 (1997) 315–334.
[18] J. Wang, T. Niioka, The effect of radiationreabsorption on NO formation in CH4/air counterflow diffusionflames, Combust. Theory Model. 5 (3) (2001) 385.
[19] X. Li, J. Zhang, J. Huo, X. Wang, L. Jiang, D. Zhao, C-shaped extinction curves and lean fuel limits of methane oxy-fuel diffusion flames at different oxygen concentrations, Fuel 259 (2020) 116296.
[20] U. Maas, J. Warnatz, Ignition processes in hydrogen- oxygen mixtures, Combust. Flame 74 (1) (1988) 53–69.
[21] U. Maas, J. Warnatz, Ignition processes in carbon-monoxide-hydrogen-oxygen mixtures, in: Symposium (International) on Combustion, vol. 22, Elsevier, 1989, pp. 1695–1704.
[22] C.K. Law, C.J. Sung, G. Yu, R.L. Axelbaum, On the structural sensitivity of purely strained planar premixed flames to strain rate variations, Combust. Flame 98 (1–2) (1994) 139–154.
[23] F.N. Egolfopoulos, Dynamics and structure of unsteady, strained, laminar premixed flames, in: Symposium (International) on Combustion, vol. 25, Elsevier, 1994, pp. 1365–1373.
[24] H. Kolla, N. Swaminathan, Strained flamelets for turbulent premixed flames, I: Formulation and planar flame results, Combust. Flame 157 (5) (2010) 943–954.